Embedding of the Brueckner expansion in the Green's function theory

C. Mahaux and R. Sartor*
Institut de Physique, Université de Liege, Sart Tilman, B-4000 Liege 1, Belgique
(Received 31 July 1978)

We discuss the relationship between the Green's function and the Brueckner expansions for the binding energy of nuclear matter. The origin of spurious-looking graphs which appear in the Green's function expansion is elucidated. Numerical values are given in the case of the Hamman-Ho-Kim nucleon-nucleon interaction. We point out the existence of a striking analogy between the Green's function and the correlated basis functions approaches.

[NUCLEAR STRUCTURE Formal and numerical comparison between the Brueckner and Green's function theories of nuclear matter.]

I. INTRODUCTION

The calculation of the average binding energy per nucleon of nuclear matter is currently subject to detailed scrutiny.[1,2] The main reason is that a discrepancy has repeatedly been exhibited between the two main available approaches: The standard version[3] of the Brueckner-Hartree-Fock (BHF) approximation yields an energy which is larger than the estimates of an upper bound obtained from various variational techniques.[1,2,4,5] This lends some support to proposals to modify[6-10] the standard BHF approximation, by attaching to the particle state with momentum b an "auxiliary" potential energy $U(b)$ which joins smoothly to that of the hole states at the Fermi momentum k_F. This reduces the so-called dispersion correction as compared to the standard BHF approximation. One of these proposals, namely, the continuous choice (3.2),[10,11] is based on a third approach, the Green's function theory of nuclear matter.[12] The latter is also interesting because it shares several features with the two other ones.

The main purpose of the present paper is threefold. Firstly, we discuss the formal relationship between the hole line expansions used in the Bethe-Brueckner theory[3] on the one hand, and in the Green's function theory[9] on the other hand. We devote special attention to the role of the auxiliary potential U. In particular, we elucidate the role of graph (C) of Fig. 1 which looks redundant (two consecutive g matrices in a particle-particle ladder) but which appears in the Green's function theory. Secondly, we illustrate the discussion with numerical calculations performed in the case of the semirealistic nucleon-nucleon interaction of Hamman and Ho-Kim.[13,14] Finally, we point out the existence of a striking analogy between the Green's function and the correlated basis function approaches.[15,16]

II. RELATIONSHIP BETWEEN THE BETHE-BRUECKNER AND THE GREEN'S FUNCTION APPROACHES

A. Basic equations

The Hamiltonian H of nuclear matter is the sum of the kinetic energy operator $T=\Sigma t(i)$ and of the two-body operator $V=\Sigma v(i,j)$. It is usually convenient to introduce an auxiliary single-particle potential $U(i)$:

$$H=H_0+H_1\,, \tag{2.1}$$

$$H_0=\sum_i\,[t(i)+U(i)]=T+U\,, \tag{2.2}$$

$$H_1=\sum_{i<j}\,[v(i,j)-U(i)]=V-U\,. \tag{2.3}$$

The potential $U(i)$ can be chosen in such a way as to optimize the rate of convergence of the various expansions, for instance that of the average binding energy per nucleon B. For simplicity, we usually shall not distinguish between binding energy and average binding energy per nucleon.

In the Bethe-Brueckner approach, one expands the quantity ΔE defined by

$$B=T_0+\Delta E$$

$$=T_0+\left\langle\Phi\left|\sum_{n=0}^{\infty}V[(E_0-H_0)^{-1}H_1]^n\right|\Phi\right\rangle_C\,, \tag{2.4}$$

where T_0 is the free kinetic energy, while E_0 is the energy in the ground state $|\Phi\rangle$ of the model Hamiltonian H_0. The subscript C means that only connected graphs should be retained in the expansion of ΔE.

In contradistinction, the Green's function theory leads to separate expansions for the kinetic energy $\langle T\rangle$ of the correlated system with wave function $|\Psi\rangle$ on the one hand, and for its interaction energy $E_{\rm int}$ on the other hand[17-19]:

$$B=\langle T\rangle+E_{\rm int}\,, \tag{2.5}$$

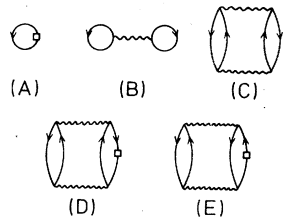

FIG. 1. Two-hole line contributions to the binding energy in the Green's function approach. The exchange graphs are not represented (see Appendix B of Ref. 19). A wiggly line corresponds to a Brueckner g matrix, and a square to a kinetic-energy insertion. All diagrams are to be computed with the ΔE rules, i.e., without any extra weighting factor (see Sec. II).

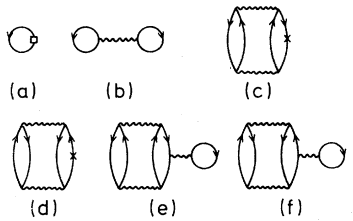

FIG. 2. Some graphs of the Bethe-Brueckner theory expansion for ΔE which are discussed in the text. Graphs (a) and (b) yield the two-hole line (BHF) contribution B_2 to the kinetic energy. Graphical conventions as in Fig. 1; a cross corresponds to a U insertion.

$$\langle T\rangle = \frac{\langle\Psi|T|\Psi\rangle}{\langle\Psi|\Psi\rangle}, \tag{2.6}$$

$$E_{\rm int} = \frac{\langle\Psi|V|\Psi\rangle}{\langle\Psi|\Psi\rangle}. \tag{2.7}$$

The expressions of $\langle T\rangle$ and of $E_{\rm int}$ can be written in terms of the Green's function $G(\vec{\mathbf{k}}, k_0)$.[20] One has for symmetric nuclear matter (spin and isospin summations carried out),

$$\langle T\rangle = -\frac{2i}{\pi}\sum_{\vec{\mathbf{k}}}\int dk_0 \frac{\hbar^2k^2}{2m} G(\vec{\mathbf{k}}, k_0), \tag{2.8}$$

$$E_{\rm int} = -\frac{i}{\pi}\sum_{\vec{\mathbf{k}}}\int dk_0\left(\hbar k_0 - \frac{\hbar^2k^2}{2m}\right)G(\vec{\mathbf{k}}, k_0), \tag{2.9}$$

where the integration contour consists of the real k_0 axis and of a semicircle in the upper halfplane.

The Green's function is related to the mass operator $M(\vec{\mathbf{k}}, k_0)$ by the Dyson equation

$$G(\vec{\mathbf{k}}, k_0) = G_0(\vec{\mathbf{k}}, k_0) + G_0(\vec{\mathbf{k}}, k_0)\left(M(\vec{\mathbf{k}}, k_0) - \frac{1}{\hbar}U(k)\right)G(\vec{\mathbf{k}}, k_0), \tag{2.10}$$

where G_0 is the Green's function of the unperturbed system described by H_0. A low-density (hole line) expansion for M was developed in Ref. 9. When substituted in Eqs. (2.8)–(2.10), this leads to an expansion for the binding energy B. The two-hole line contribution to this expansion derived in Ref. 9 is represented by graphs (A) to (E) of Fig. 1, where a square corresponds to the insertion of the kinetic energy $\hbar^2k^2/2m$ and a wiggly line to the reaction matrix g of Brueckner's theory. Following Ref. 19, we do not draw the exchange graphs. Graph (A) yields the unperturbed energy T_0. Graphs $(A)+(B)$ give the BHF approximation B_2 [$=(a)+(b)$ in Fig. 2] for B. Graphs (D) and (E) give the leading contribution to the difference between the kinetic energy $\langle T\rangle$ of the correlated system and that, T_0, of the free Fermi gas,

$$\langle T\rangle - T_0 \simeq (D)+(E) = \tfrac{1}{2}\sum \frac{|\langle a,b|g|j,l\rangle_A|^2}{[e(a)+e(b)-e(j)-e(l)]^2} \times\left(\frac{\hbar^2a^2}{2m}-\frac{\hbar^2l^2}{2m}\right), \tag{2.11}$$

where the index A refers to antisymmetrization: $|j,l-l,j\rangle = |j,l\rangle_A$. Here and below, $a,b,\ldots$ and $j,l,\ldots$ refer to particle and to hole states, respectively.

B. Origin of spurious-looking graphs

Graph (C) has a spurious appearance since it involves two consecutive g interactions in a particle-particle ladder. Its expression reads (a factor $\frac{1}{2}$ is missing in Ref. 9)

$$(C) = \tfrac{1}{4}\sum \frac{|\langle a,b|g|jl\rangle_A|^2}{e(j)+e(l)-e(a)-e(b)}, \tag{2.12a}$$

with

$$e(k) = \hbar^2k^2/2m + U(k). \tag{2.12b}$$

The existence of this graph (C) can be understood in the following way. Consider the linked cluster expansion[19] of $E_{\rm int}$,

$$E_{\rm int} = \left\langle\Phi\right|\sum_{p=0}^{\infty}[H_1(E_0-H_0)^{-1}]^pV \times\sum_{q=0}^{\infty}[(E_0-H_0)^{-1}H_1]^q\left|\Phi\right\rangle_C. \tag{2.13}$$

By comparing this expression with the corresponding one [see Eq. (2.4)] for ΔE, it can be checked that a Goldstone diagram N for $E_{\rm int}$ will be computed by using the same rules as those for E except for an extra weighting factor equal to the

number n_v of v interactions contained in N. Indeed, consider for instance a diagram N_3 for ΔE "generated" by the term

$$V(E_0 - H_0)^{-1} U(E_0 - H_0)^{-1} V(E_0 - H_0)^{-1} V$$

in (2.4). This term appears $n_v = 3$ times in the expansion (2.13), namely, for $p=0$, $q=3$ and $p=2$, $q=1$ and $p=3$, $q=0$. This example illustrates that any v interaction in a diagram for ΔE can be used as a separator between the sums over p and q in (2.13), whence the extra factor n_v for the E_{int}-diagrams.

Consider now the Brueckner ladder summation which leads to the contribution to ΔE respresented by graph (b) of Fig. 2. This ladder summation yields graphs (B) and (C) for E_{int}. This is demonstrated in a picturesque way in Fig. 3. All diagrams shown there should be computed with the ΔE rules: The n_v factor is explicitly written in Fig. 3 in front of each diagram.

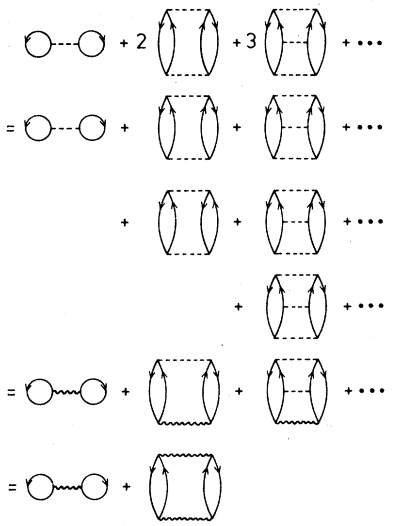

FIG. 3. A graphical computation of the two-hole line contribution $E_{\text{int}}^{(2)}$ to the interaction energy in nuclear matter. A horizontal dashed line represents a v interaction, a wiggly line denotes a g matrix. All diagrams are to be computed with the ΔE rules (Ref. 27), the n_v weighting factors are written explicitly.

C. Role of spurious-looking graphs

We now show that the spurious-looking graphs, of which graph (C) of Fig. 1 is an example, correspond to the inclusion, in the n-hole line term of the Green's function expansion of $\langle T\rangle + E_{\text{int}}$, of some dispersion-diagrams which appear in higher-order terms of the Bethe-Brueckner expansion for ΔE.

The sum of the graphs (A) to (E) in Fig. 1 takes the following simple form:

$$(A)+\cdots+(E) = B_2 + \tfrac{1}{2}\sum \frac{|\langle a,b|g|j,l\rangle_A|^2}{[e(a)+e(b)-e(j)-e(l)]^2} \times [U(l)-U(a)]\,. \qquad (2.14)$$

Let us denote by ΔU the second term on the right-hand side of Eq. (2.14). It is a negative quantity for any sensible choice of $U(k)$, i.e., one which is such that U (particles) $> U$ (holes). It is a "dispersion term" in the sense that it vanishes if $U(k)$ is independent of k.

It thus appears from Eq. (2.14) that at the two-hole line level the Green's function theory yields a smaller energy (more binding) than the BHF approximation B_2, where the difference is the dispersion term. This reminds us of a very similar difference that exists between the BHF approximation B_2 on the one hand and the two-body cluster estimate $E_{[2]}$ of $\langle\Psi|H|\Psi\rangle/\langle\Psi|\Psi\rangle$ on the other hand: One has[21-23]

$$E_{[2]} = B_2 + \Delta U\,, \qquad (2.15)$$

for a suitable choice of the correlation operator F defined by $\Psi = F\phi$. The BHF approximation B_2 thus lies *above* the approximate upper bound $E_{[2]}$, which leads to the discrepancy alluded to at the beginning of this paper. The problem consists of determining whether ΔU is a "spurious" contribution to the Brueckner-Hartree-Fock or to the two-body cluster approximation to the upper bound. The truth probably lies somewhere between these two extremes and depends on the choice of $U(k)$. The same problem arises when comparing the two-hole line approximations of the Green's function and of the Bethe-Brueckner expansions. We now discuss it in some detail.

Let us go back to expression (2.14). It can be seen by direction computation that ΔU, i.e., the sum of diagrams (C)–(E) of Fig. 1, is precisely equal to the ΔE graphs (c) and (d) of Fig. 2,

$$(A)+(B)+(C)+(D)+(E) = (a)+(b)+(c)+(d)\,. \qquad (2.16)$$

This suggests that the Green's function approach is "some" dispersion diagrams ahead of the Bethe-Brueckner theory. We now show that this is a general feature of the Green's function approach.

D. Generalization

Consider the sum of the diagrams (a) and (b) of Fig. 4. Diagram (a) is to be computed with the ΔE rules; diagram (b) is a sum over the diagrams obtained from (a) by making a kinetic energy insertion in every fermionic line encountered by the horizontal bar. No redundancy problem arises if one counts the pairs of equivalent lines in (b) in the same way as in (a), i.e., disregarding the square insertions. Let us call M the expression

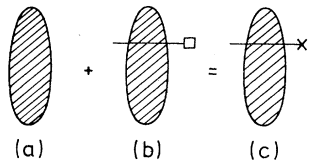

FIG. 4. Elimination of $\langle T\rangle$ diagrams by $E_{\rm int}$ diagrams. Graphs (*b*) and (*c*) are sums over the diagrams obtained by making square (kinetic energy) and cross (potential energy) insertions in every fermionic line encountered by the horizontal bar. Diagrams (*a*) and (*c*) are computed with the ΔE rules.

common to diagrams (*a*), (*b*), and (*c*). Using the conventions of Ref. 19, one finds

$$(a)+(b)=\sum \frac{M}{\Sigma e_< - \Sigma e_>}(\Sigma e_< - \Sigma e_> + \Sigma t_> - \Sigma t_<)$$

$$=\sum\left[\frac{M}{\Sigma e_< - \Sigma e_>}(\Sigma U_< - \Sigma U_>)\right]$$

$$= \text{diagram } (c) \text{ of Fig. 4}. \qquad (2.17)$$

Here, the subscripts < and > refer to holes and to particles, respectively; the summations within the square brackets run over the lines encountered by the horizontal bars of diagrams (*b*) and (*c*) while the outer summation is the familiar one over momenta, spin, and isospin. The redundancy problems in diagram (*c*) are taken care of as in diagram (*b*). The weighting factors associated with each diagram must be discussed in some detail.

If diagram (*a*) of Fig. 4 contains n interactions, it can be matched with $n-1$ diagrams of type (*b*). In the $E_{\rm int}$ expansion, diagram (*a*) is multiplied by a factor n_v, where n_v is the number of two-body interactions that it contains. If we call n_U the number of U interactions in diagram (*a*), this means that $n-1-n_V=n_U-1$, diagrams of type (*a*) are lacking to use up all the (*b*) diagrams as described in Eq. (2.17). However, the procedure depicted in Fig. 4 can be applied to the n_U diagrams (*a'*) of order $n-1$ which are obtained from (*a*) by suppressing each U interaction in turn. By matching n_U-1 of these (*a'*) diagrams with the *ad hoc* (*b'*) diagrams, one generates n_U-1 (*c'*) diagrams which coincide with the (*a*) diagrams. Hence, all (*b*) diagrams will be used up. One will remain with only one (*a*) diagram computed with the ΔE rules and a series of (*c*) diagrams which can easily be written out explicitly in each particular case.

We conclude that a given subset Z of graphs in the Bethe-Brueckner theory will formally be identical to the corresponding subset in the Green's function theory (i.e., the subset of $E_{\rm int}$ and $\langle T\rangle$ diagrams with the same topology as the ΔE diagrams in Z) only if Z contains along with any diagram N, the diagrams obtained by making a selected number of U insertions in N.

The cancellation represented in Fig. 4 generates (*c*) graphs with U insertions in hole as well as in particle lines. This may raise some ambiguity as far as counting the number of hole lines in the expansions is concerned, since a U insertion should normally be counted as a hole line. We already encountered this feature when we pointed out that the two-hole line $E_{\rm int}$ diagrams $(C)+(D)+(E)$ (see Fig. 1) generates the ΔE diagrams (*c*) and (*d*) of Fig. 2. Diagram (*c*) of Fig. 2 is customarily included in the class of three-hole line diagrams since it cancels diagram (*e*) (Fig. 2) when U is chosen self-consistently for hole states. When the self-consistency is extended to particle states, diagram (*d*) (Fig. 2) should also formally be considered as a three-hole line diagram while if one adopts Brandow's prescription,[18,24] it should rather be included in the class of four-hole line diagrams. In the standard prescription[3] (3.1), graph (*d*) vanishes identically.

E. U insertions in the Green's function expansion

Equation (2.16) shows that the sum of all the one- and two-hole line graphs in the Green's function expansion for $B=\langle T\rangle+E_{\rm int}$ is equal to the sum $(a)+(b)$ (Fig. 2) of the one- and two-hole line graphs (*c*) and (*d*) (Fig. 2), which are usually counted as three-hole line graphs. This raises two problems. The first one consists of finding out whether this anticipation of dispersive correcrections is an advantage or a drawback of the Green's function expansion. We discuss this point in Sec. III. The second problem is that one may wonder whether a double-counting problem does not occur in the Green's function expansion, since graphs analogous to (*c*) and (*d*) (Fig. 2) will also exist there, in addition to being hidden in graphs (*A*) to (*E*). We now demonstrate, with the help of an example, that the weighting factors automatically take care of this apparent double-counting.

Let us consider the subset Z of ΔE diagrams represented by the diagrams (*a*), (*b*), (*c*), and (*e*) of Fig. 2. With the self-consistent choice for the hole potential, one has

$$(a)+(b)+(c)+(e)=(a)+(b)\,. \qquad (2.18)$$

The corresponding subset Z' of Green's function theory diagrams includes the graphs shown in Fig. 1 plus all the diagrams of Fig. 5 where we have explicitly written the weighting factors. These diagrams correspond to the three-hole line graphs included in Z. Notice the spurious-looking dia-

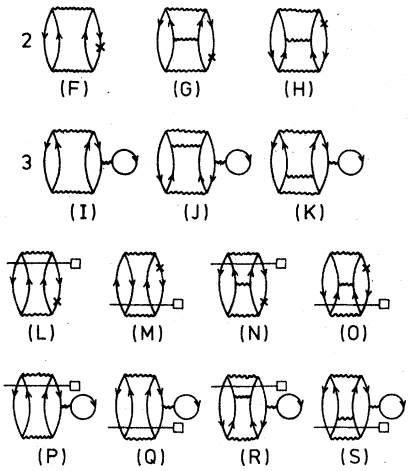

FIG. 5. Three hole line $\langle T\rangle$ and $E_{\rm int}$ diagrams which correspond to the ΔE diagrams (c) and (e) of Fig. 2, i.e., which are obtained by making a U or a bubble insertion in a hole line of a two-hole line diagram. The meaning of the horizontal bar is explained in Fig. 4.

grams (G), (H), (J) and (K).

If one uses a self-consistent auxiliary potential for hole states, one has

$$(F)+(I)=(e)\ \text{(Fig. 2)}, \tag{2.19}$$

while all other diagrams cancel in pairs, for instance,

$$(G)+(J)=0\,. \tag{2.20}$$

Hence, it follows that

$$[(A)+\ldots+(E)]\ \text{(Fig. 1)}+[(F)+\ldots+(S)]\ \text{(Fig. 5)} = [(a)+\ldots+(e)]\ \text{(Fig. 2)}\,. \tag{2.21}$$

This shows that the addition of (c)- and (e)-type diagrams to both expansions changes their difference from $(c)+(d)$ (Fig. 2) to (d) (Fig. 2). The latter vanishes for the standard auxiliary potential (3.1) ($U=0$ for particle states).

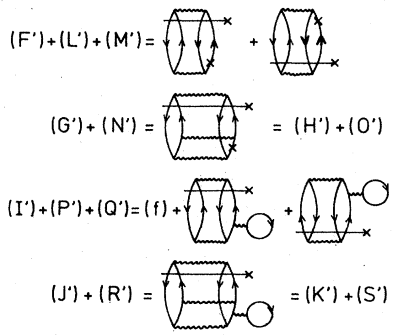

FIG. 6. Sums of graphs analogous to the unprimed ones shown in Fig. 5, except that the U or bubble insertions are made on particle rather than on hole lines. The symbol (f) refers to graph (f) of Fig. 2.

In order to be consistent with the spirit of hole line expansions, all three-hole line diagrams should be included in Z. As a formal first step in this direction, one should include the diagrams analogous to diagram (f) of Fig. 2 in both expansions. When one adopts the continuous prescription (3.2) for the auxiliary potential U, diagrams of type (d) in Fig. 2 should also be considered as a three-hole line diagram. These graphs can be grouped as indicated by the equations depicted in Fig. 6. There, (F')–(S') are diagrams similar to diagrams (F)–(S) of Fig. 5, with the only difference that the U and the bubbles are inserted in particle rather than in hole lines. Equation (2.21) is now replaced by

$$[(A)+\cdots+(E)]+[(F)+\cdots+(S)]+[(F')+\cdots+(S')] = [(a)+\cdots+(f)]+R\,, \tag{2.22}$$

where R is the sum of all dispersion diagrams shown in Fig. 6. We note that in the present case R does not vanish even for the standard auxiliary potential.

III. CONVERGENCE OF THE EXPANSIONS

We have shown in Sec. II that the hole-line expansions for the binding energy obtained from the Green's function and Brueckner approaches, respectively, are two distinct rearrangements of the linked-cluster perturbation series. These two expansions differ by only a small number of graphs for a given order in the number of hole lines. This is illustrated by the examples (2.16) and (2.22). The rates of convergence of the two expansions should therefore be rather similar. Nevertheless, the difference may be significant in practice, since one is limited to the computation of the leading terms of the expansions.

Let us accordingly concentrate our discussion on these terms, more specifically on the graphs shown in Figs. 1 and 2, for which we shall give numerical values in Sec. IV. The relevant relations in this context are Eqs. (2.14), (2.16), and (2.22). They show that the main difference between the two expansions are very closely connected with the existence of an auxiliary potential U. If U could be set equal to zero, the n-hole line spurious-looking graphs of the Green's function expansion would cancel the n-hole line diagrams which represent the difference $\langle T\rangle - T_0$, and one would then recover the Bethe-Brueckner expansion order by order. However, the convergence of the hole-line expansions appear to require the introduction of a nonvanishing auxiliary potential, although other expansions have been proposed which avoid its use.[6]

Two choices for the auxiliary potential have been alluded to above. These are, respectively, the "standard choice" defined by[3]

$$U(k)=\begin{cases}\sum_j \langle j,k|g|j,k\rangle_A, & \text{for } k<k_F\\ 0, & \text{for } k>k_F\end{cases} \tag{3.1}$$

and the "continuous choice" defined by[9]

$$U(k)=\sum_j \langle j,k|g|j,k\rangle_A, \quad \text{for all } k. \tag{3.2}$$

In the Green's function expansion, the two-hole line approximation is given by the sum of the diagrams (A) to (E) in Fig. 1. This is equal to the sum of the graphs (a) to (d) in Fig. 2. We recall that $B_2=(a)+(b)$ is the BHF approximation. Graphs (c) and (d) are dispersion diagrams whose sum ΔU is the second term on the right-hand side of Eq. (2.14).

Equation (2.16) shows that the Green's function expansion "anticipates" the dispersion graphs of the Bethe-Brueckner expansion. At first sight, this is not an advantage. Indeed, the dispersion graph (c), for instance, is exactly cancelled by graph (e) in the Bethe-Brueckner expansion. This is true for the two choices (3.1) and (3.2) of $U(k)$. Thus it appears undesirable to treat graph (c) separately from graph (e). Actually, the situation is more delicate than it seems. In order to exhibit this, we first discuss graph (c) and then turn to graph (d).

Dispersion effects already exist in a somewhat hidden form in graph $(b)=(B)$ which corresponds to the BHF approximation. Indeed, the g matrix used there is quite sensitive to the fact that the choices (3.1) and (3.2) increase the energy difference between particle and hole states, especially in the case of the standard choice (3.1). It is this dispersion effect that has been taken to be responsible for the discrepancy (2.15) between the standard version of the BHF approximation and variational calculations.[1,2,23,25] The dispersion graph (c) strongly reduces this dispersion effect contained in (b). Thus variational calculations suggest that it is desirable to group graph (c) with graph (b) rather than with (e) in the ordering of the series. However, this point is far from settled.

A related problem concerns graphs (d) and (f) (Fig. 2). Graph (d) vanishes for the standard choice (3.1). It is different from zero for the continuous choice (3.2), for which it is believed to cancel a significant fraction of the contribution of graph (f).[8,10,11] We also note that the sign of (d) is opposite to that of (c) (see Sec. IV). Hence, the sum $(c)+(d)$ is smaller for the continuous choice than for the standard one. The latter leaves (f) uncanceled and groups it with the other three-hole diagrams although this may be inconvenient for particle momenta close to k_F.[8] The variational approach suggests that graph (f) is almost as important as graph (e).[23] This is also one of the arguments which underlie the continuous prescription (3.2). It has, moreover, been argued that the latter is such that graph (e) cancels most of the sum of *all* three-hole line graphs in the Bethe-Brueckner expansion.[10]

We realize that this discussion becomes cumbersome; this reflects the intricacy of the problem of finding the "best choice" for the auxiliary potential and of performing the selection of the dominant graphs. The safest procedure consists in including enough graphs so that their sum becomes almost independent of the choice of the auxiliary potential U. This appears to be achieved at the three-hole line level,[1,26] but the sum of the three-hole line graphs is very hard to calculate in a reliable way in the case of realistic interactions. Thus it is of great practical interest to find a choice for U which yields an accurate version of a lower order approximation. In the absence of any clear-cut argument, we can only list a few alternatives, and risk value judgments which are admittedly somewhat subjective or prejudiced.

We believe that the sum (2.16),

$$\begin{aligned}S_1&=(A)+(B)+(C)+(D)+(E)\\&=(a)+(b)+(c)+(d),\end{aligned} \tag{3.3}$$

gives a rather good approximation to the binding energy, for the following reasons. We first notice that this sum depends only weakly on the choice of U, because of the large cancellation between the dispersion effects contained in (b) on the one hand, and in (c) and (d) on the other hand.[26] Secondly, this approximation appears quite naturally in the framework of the Green's function approach.[9] Thirdly, the approximation S_1 removes the discrepancy between the variational methods and the hole line expansions [see Eq. (2.15)]. In order to obtain an accurate result, it is nevertheless advisable to add to S_1 the graphs (e), (f), and the sum of all the other three-hole line graphs, as well as the dominant four-hole line (renormalization) diagram. However, we believe that the three-hole line correction is fairly small because the repulsive graph (e) approximately cancels the sum of the other three-hole line graphs.[1,27]

Arguments put forward in Refs. 10–12 indicate that graph (d) cancels a significant portion of the sum of all three-hole line graphs other than (e) provided that the continuous choice (3.2) is adopted. For the latter choice, the BHF expression

$$S_2 = (a) + (b) + (c) + (e)$$
$$= (a) + (b) = B_2 \tag{3.4}$$

therefore appears to be a reasonable approximation to the binding energy. It has the important advantage over S_1 of being much easier to calculate. We emphasize that the BHF approximation S_2 is probably not accurate in the case of the standard choice (3.1). Then indeed, graph (d) vanishes and one should add to S_2 the diagram (f) and the sum of the other three-hole line graphs. This is a large negative quantity[1] which, as noted above, is approximately canceled by graph (e). We conclude that the simple BHF approximation (3.4) is at least as good as the more complicated expression (3.3) in the case of the continuous choice. In contradistinction, expression S_2 yields a significant underbinding in the conventional version of the BHF approximation,[3] which is based on the standard choice (3.1).

The sum of all graphs shown in Fig. 2 reads

$$S_3 = (a) + (b) + (c) + (d) + (e) + (f)$$
$$= (a) + (b) + (d) + (f), \tag{3.5}$$

where the last eqality holds for the standard as well as for the continuous choices (3.1) and (3.2). Its accuracy seems comparable to that of S_1.

In summary, it appears that the approximations S_1, S_2, and S_3 have similar accuracy, provided that the continuous choice (3.2) is adopted in the case of S_2. We believe that with this choice for U the BHF approximation S_2 may even be more accurate than S_1 or S_3 while being, moreover, much simpler from the computational point of view. In any case, the difference between the values of S_1, S_3, and S_2 (with the continuous choice) gives a measure of their accuracy; one should in addition not forget the existence of at least one large four-hole line (renormalization) graph.

IV. NUMERICAL VALUES

We computed the value of the graphs shown in Figs. 1 and 2, except that of (f), in the case of the semirealistic nucleon-nucleon interaction of Hamman and Ho-Kim[13,14] and of the continuous choice (3.2). The Fermi momentum k_F has been taken equal to 1.36 fm^{-1}.

The results are listed in Table I. They can be calculated from the quantities calculated in Refs. 28 and 29. Diagram (C) is intimately related to the rearrangement contribution to the optical potential, diagrams (D) and (E) can be derived from the momentum distributions given in Ref. 29. Diagram (e) can be obtained from the momentum distribution below k_F and from the one-hole line contribution $v^{(1)}$ to the optical-model potential. Indeed, one has

TABLE I. Contribution to the average binding energy per nucleon of some diagrams shown in Figs. 1 and 2, for $k_F = 1.36$ fm^{-1} and for the continuous choice of the auxiliary potential. Antisymmetrization is included. The nucleon-nucleon interaction is due to Hamman and Ho-Kim (Ref. 13).

Graph	Value (MeV/nucleon)
$(a) = (A)$	23
$(b) = (B)$	−48.75
(c)	−8.15
(d)	5.3
(e)	8.15
(C)	−7.15
(D)	−2.3
(E)	6.6

$$(e) = -\tfrac{1}{2}\sum \frac{|\langle a,b|g|j,l\rangle_A|^2}{[e(a)+e(b)-e(j)-e(l)]^2} \times \langle j,l|g|j,l\rangle_A$$
$$= \sum \rho_<^{(1)}(l) v^{(1)}(l), \tag{4.1}$$

where $\rho_<^{(1)}(l)$ is the leading correction to the Fermi momentum distribution below k_F. The value of the diagrams (c) and (d) can then be found by using Eq. (2.16) and the cancellation between diagrams (c) and (e).

We note that diagram (d) is positive. This can be understood from the expression

$$(d) = -\tfrac{1}{2}\sum \frac{|\langle a,b|g|j,l\rangle_A|^2}{[e(j)+e(l)-e(a)-e(b)]^2} U(b)$$
$$= -\sum \rho_>^{(2)}(b) U(b). \tag{4.2}$$

Here, the positive quantity $\rho_>^{(2)}(b)$ is the leading correction to the Fermi momentum distribution above k_F. In Ref. 29, it is found that $\rho_>^{(2)}(b)$ is a rapidly decreasing function of b, from which it follows that the main contribution to (4.2) arises from the domain of values for b where $U(b)$ is negative [$U(k_F) \simeq -70$ MeV for the Hamman–Ho-Kim interaction]. Hence, the sign of contribution (d) will probably be positive for any realistic nucleon-nucleon interaction, for the continuous prescription for the auxiliary potential. With the prescription of Ref. 18 for $U(b)$, diagram (d) would be negative and very small in magnitude. Indeed, the corresponding $U(b)$ is equal to the real part of the rearrangement contribution to the optical potential, which is equal to approximately +7 MeV for b close to k_F. However, one should keep in mind that graph (b) is also affected by a change in the definition of $U(a)$ for particle states, and that the sum $(b)+(c)+(d)$ probably does not

depend much on the choice of the auxiliary potential.[26]

We are now in a position to compute the approximations S_1 and S_2. The BHF approximation yields

$$S_2 = -25.75 \text{ MeV/nucleon}, \tag{4.3}$$

while the two-hole line approximation of the Green's function expansion gives

$$S_1 = -28.6 \text{ MeV/nucleon}. \tag{4.4}$$

As described in Secs. IIC and III, the difference between S_1 and S_2 is due to the dispersion graphs (*c*) and (*d*) and gives a rough measure of the accuracy of both approximations. This difference would be much larger in the case of the standard choice (3.1).

V. ANALOGY BETWEEN THE GREEN'S FUNCTION AND THE VARIATIONAL APPROACHES

The Bethe-Brueckner theory is based on the expansion of the matrix element $\langle\phi|H|\Psi\rangle$. The Green's function theory deals with the expectation value $\langle\phi|H|\Psi\rangle$. It is in this respect closer to the variational approach, where the true ground state Ψ is approximated by a trial wave function.

We now briefly point out a striking analogy that exists between the two-hole line approximation to the Green's function expansion on the one hand and the two-body cluster approximation of the correlated basis function approach[15,30] on the other hand. For the latter, we adopt the notation of Refs. 16, 31, and 32. There the binding energy is written in the form

$$B \simeq E_{[2]} + (\delta E)^{(2)}, \tag{5.1}$$

with

$$E_{[2]} = T_0 + \tfrac{1}{2}\sum \langle j,l|w_2|j,l\rangle_A . \tag{5.2}$$

The quantity w_2 plays the role of an effective interaction. However, no auxiliary potential is introduced in the variational approach, whence the difference between $E_{[2]}$ and $S_2 = B_2$ expressed by Eq. (2.15). The latter relation and Eq. (3.3) show that

$$S_1 \simeq E_{[2]}. \tag{5.3}$$

In the correlated basis function approach, the correction $(\delta E)^{(2)}$ in Eq. (5.1) is evaluated in second-order perturbation theory; it then reads

$$(\delta E)^{(2)} = \tfrac{1}{4}\sum \frac{|[\langle a,b|w_2|j,l\rangle_A + \frac{1}{2}(\epsilon_a+\epsilon_b-\epsilon_j-\epsilon_l)\langle a,b|\eta|j,l\rangle_A]|^2}{\epsilon(j)+\epsilon(l)-\epsilon(a)-\epsilon(b)}, \tag{5.4}$$

where

$$\epsilon(k) = \frac{\hbar^2k^2}{2m} + \sum_j \langle k,j|w_2|k,j\rangle_A \tag{5.5}$$

can be identified with $e(k)$ [Eq. (2.12b)]. The second term in the square brackets in the numerator of (5.4) is a nonorthogonality correction which diminishes the absolute value of the content of the brackets. The first term in the square brackets gives rise to the contribution

$$\tfrac{1}{4}\sum \frac{|\langle a,b|w_2|j,l\rangle_A|^2}{\epsilon(j)+\epsilon(l)-\epsilon(a)-\epsilon(b)}, \tag{5.6}$$

which is formally identical to the expression (2.12a) of graph (*C*) in Fig. 1. It appears difficult to find a correspondence between the nonorthogonality correction and the Green's function expansion. We note that its sign is such that it helps cancel the difference ΔU between (*A*)+(*B*) of Fig. 1 and $E_{[2]}$ [Eq. (2.15)]. This suggests that the correlated basis function approximation (5.1) yields a result close to the sum of the graphs (*A*), (*B*), and (*C*) of Fig. 1.

VI. CONCLUSIONS

In Sec. II, we have shown that a close relationship exists between the hole-line expansions derived from the Green's function and from Brueckner's theories, respectively. We have formally justified the appearance in the former approach of spurious-looking graphs, and we have discussed their physical role. The comparison between the two expansions sheds some light on the appropriate way of choosing the auxiliary potential $U(k)$, which appears as a parameter in both approaches (Sec. III).

In the two-hole line approximation, the Green's function theory yields more binding than the Bethe-Brueckner approach, especially than the conventional version of the Brueckner-Hartree-Fock approximation. The variational approach indicates that this is a favorable property. Numerical examples are given in Sec. IV.

The Green's function approach has a striking formal analogy to the variational approach, to which it appears closer than the Bethe-Brueckner expansion (Sec. V). It also indicates the utility

of treating particle and hole intermediate states on the same footing.

We thank the authors of Ref. 23 for inspiring the title of this paper.

---

*Chercheur I. I. S. N.

[1]B. D. Day, Rev. Mod. Phys. 50, 495 (1978).
[2]J. W. Clark, Progr. Part. Nucl. Phys. (to be published), and references contained therein.
[3]H. A. Bethe, Annu. Rev. Nucl. Sci. 21, 93 (1971).
[4]S.-O. Bäckman, D. A. Chakkalakal, and J. W. Clark, Nucl. Phys. A130, 635 (1969).
[5]S.-O. Bäckman, J. W. Clark, W. J. Ter Louw, D. A. Chakkalakal, and M. L. Ristig, Phys. Lett. 41B, 247 (1972).
[6]G. A. Baker, Jr., Rev. Mod. Phys. 43, 479 (1971), and references contained therein.
[7]H. S. Köhler, Nucl. Phys. A128, 273 (1969).
[8]H. S. Köhler, Nucl. Phys. A204, 65 (1973).
[9]J. Hüfner and C. Mahaux, Ann. Phys. (N.Y.) 73, 525 (1972).
[10]J.-P. Jeukenne, A. Lejeune, and C. Mahaux, Nucl. Phys. A245, 411 (1975).
[11]A. Lejeune and C. Mahaux, Nucl. Phys. A295, 189 (1978).
[12]J.-P. Jeukenne, A. Lejeune, and C. Mahaux, Phys. Rep. 25C, 83 (1976).
[13]T. F. Hamman and Q. Ho-Kim, Nuovo Cimento 64B, 356 (1969).
[14]Q. Ho-Kim and R. Provencher, Nuovo Cimento 14A, 633 (1973).
[15]J. W. Clark and P. Westhaus, Phys. Rev. 141, 833 (1966); 149, 990 (1966).
[16]J. W. Clark, P. M. Lam, and W. J. Ter Louw, Nucl. Phys. A255, 1 (1975).
[17]R. Prange and A. Klein, Phys. Rev. 112, 1008 (1958).
[18]B. H. Brandow, Phys. Rev. 152, 863 (1966).
[19]B. H. Brandow, Rev. Mod. Phys. 39, 771 (1967).
[20]A. A. Abrikosov, L. P. Gorkov and I. E. Dzyaloshinsky, *Methods of Quantum Field Theory in Statistical Physics* (Prentice Hall, Englewood Cliffs, New Jersey, 1963).
[21]C. W. Wong, Phys. Rev. C 3, 1058 (1971).
[22]C. W. Wong, Phys. Rev. Lett. 26, 783 (1971).
[23]J. W. Clark and M. L. Ristig, Phys. Rev. C 7, 1792 (1973).
[24]D. S. Koltun, Phys. Rev. C 9, 484 (1974).
[25]V. R. Pandharipande, R. B. Wiringa and B. D. Day, Phys. Lett. 57B, 205 (1975).
[26]C. Mahaux, Nucl. Phys. A163, 299 (1971).
[27]B. D. Day, Rev. Mod. Phys. 39, 719 (1967).
[28]R. Sartor, Nucl. Phys. A267, 29 (1976).
[29]R. Sartor, Nucl. Phys. A289, 329 (1977).
[30]J. W. Clark and E. Feenberg, Phys. Rev. 113, 388 (1959).
[31]K. E. Kürten, M. L. Ristig, and J. W. Clark, Phys. Lett. 74B, 153 (1978).
[32]K. E. Kürten, M. L. Ristig, and J. W. Clark, Nucl. Phys. (to be published).